Development 126, 1397-1406 (1999)
Printed in Great Britain © The Company of Biologists Limited 1999
DEV1373

Krox-20 controls SCIP expression, cell cycle exit and susceptibility to apoptosis in developing myelinating Schwann cells

Todd S. Zorick[1,2], Daniel E. Syroid[1], Adrienne Brown[1], Tom Gridley[3] and Greg Lemke[1,*]

[1]Molecular Neurobiology Laboratory, The Salk Institute, La Jolla, CA 92037, USA
[2]Department of Neurosciences, UC San Diego, La Jolla, CA 92093, USA
[3]The Jackson Laboratory, Bar Harbor, ME 04609, USA
*Author for correspondence (e-mail: lemke@salk.edu)

Accepted 14 January; published on WWW 3 March 1999

SUMMARY

The transcription factors Krox-20 and SCIP each play important roles in the differentiation of Schwann cells. However, the genes encoding these two proteins exhibit distinct time courses of expression and yield distinct cellular phenotypes upon mutation. SCIP is expressed prior to the initial appearance of Krox-20, and is transient in both the myelinating and non-myelinating Schwann cell lineages; while in contrast, Krox-20 appears ~24 hours after SCIP and then only within the myelinating lineage, where its expression is stably maintained into adulthood. Similarly, differentiation of *SCIP*$^{-/-}$ Schwann cells appears to transiently stall at the promyelinating stage that precedes myelination, whereas *Krox-20*$^{-/-}$ cells are, by morphological criteria, arrested at this stage. These observations led us to examine SCIP regulation and Schwann cell phenotype in Krox-20 mouse mutants. We find that in *Krox-20*$^{-/-}$ Schwann cells, SCIP expression is converted from transient to sustained. We further observe that both Schwann cell proliferation and apoptosis, which are normal features of SCIP^{+} cells, are also markedly increased late in postnatal development in Krox-20 mutants relative to wild type, and that the levels of cell division and apoptosis are balanced to yield a stable number of Schwann cells within peripheral nerves. These data demonstrate that the loss of Krox-20 in myelinating Schwann cells arrests differentiation at the promyelinating stage, as assessed by SCIP expression, mitotic activity and susceptibility to apoptosis.

Key words: Krox-20, Schwann cell, Apoptosis, SCIP, Myelination, Mouse

INTRODUCTION

Myelination of peripheral nervous system (PNS) axons is carried out by Schwann cells, whose origins in the neural crest and subsequent differentiation in peripheral nerves have been extensively studied at both the morphological and molecular levels (for reviews, see Mirsky and Jessen, 1996; Zorick and Lemke, 1996; Taylor and Suter, 1997). It is now appreciated that Schwann cell precursors migrate and proliferate along pre-existing axon tracts during development and progress through distinct developmental stages that are marked by the acquisition of new, or the loss of pre-existing, molecular markers (Blanchard et al., 1996; Jessen et al., 1994). By the time of birth in rodents, Schwann cells destined to myelinate can be distinguished by a 'promyelinating' morphology, in which individual cells have synthesized a basal lamina and have established a 1:1 relationship of Schwann cell to axon, but have not yet initiated myelin membrane biosynthesis, wrapping or compaction (Friede and Samorajski, 1968; Martin and Webster, 1973; Webster et al., 1973). The number of promyelinating Schwann cells is greatest on the day of birth in the rat, and subsequently declines as these cells differentiate (Friede and Samorajski, 1968). Early promyelinating cells, which are sometimes referred to as 'premyelinating Schwann cells' (Zorick and Lemke, 1996), are still capable of division, whereas the onset of myelination is associated with final but not irreversible withdrawal from the cell cycle (Friede and Samorajski, 1968).

Recently, we and others have demonstrated that the promyelinating phase is also characterized by Schwann cell apoptosis, which is most evident in rodent peripheral nerves during the first two weeks after birth, and which markedly declines in the adult (Grinspan et al., 1996; Nakao et al., 1997; Syroid et al., 1996). This apoptosis is controlled by axonal contact and is in part regulated by neuregulin-1 that is supplied by the ensheathed axons (Grinspan et al., 1996; Syroid et al., 1996; Trachtenberg and Thompson, 1996). The promyelinating-to-myelinating transition is therefore characterized by changes in mitotic activity and susceptibility to apoptosis that together match the number of Schwann cells in a given peripheral nerve to the number of existing axons.

Two transcription factors have been shown to be important regulators of the promyelinating-to-myelinating transition. The first of these is the POU domain protein SCIP (Oct-6/Tst-1). SCIP expression in Schwann cells is transient: it is induced by contact with axons, is maximal in promyelinating cells that

retain the capacity to divide, is gradually extinguished as cells begin to elaborate the myelin organelle and is nearly undetectable in rodent peripheral nerves by the end of the second postnatal week (Monuki et al., 1990; Scherer et al., 1994; Zorick et al., 1996). The protein is also strongly and rapidly upregulated in cultured Schwann cells by agents that elevate intracellular cAMP (e.g., forskolin, cAMP analogs; Monuki et al., 1989, 1990), a manipulation that in many respects yields cultured cells with the molecular phenotype of promyelinating cells in vivo. The second transcription factor of demonstrated importance to the onset of myelination is the zinc finger protein Krox-20 (Egr-2). In contrast to SCIP, Schwann cell expression of Krox-20 is evident in promyelinating cells only ~24 hours after these cells first become $SCIP^+$. This expression is thereafter maintained throughout the course of myelination (which extends for more than a week in rodent nerves) and into adulthood (Blanchard et al., 1996; Zorick et al., 1996). Within the myelinating Schwann cell lineage, the progression from early promyelinating to late promyelinating to myelinating cells therefore corresponds to the phenotypic progression $SCIP^+Krox\text{-}20^-$ to $SCIP^+Krox\text{-}20^+$ to $SCIP^-Krox\text{-}20^+$. This applies only to the myelinating lineage, since Krox-20 expression is restricted to this lineage, whereas transient SCIP expression is a developmental feature of both myelinating and non-myelinating Schwann cells (Blanchard et al., 1996; Zorick et al., 1996).

Preliminary studies of the Schwann cell phenotypes in mice carrying engineered mutations in the *SCIP* and *Krox-20* genes have highlighted the importance of these differential patterns of developmental regulation to Schwann cell differentiation. Schwann cells in the peripheral nerves of $SCIP^{-/-}$ mice, for example, exhibit a striking defect in differentiation. This defect was thought to reflect an arrest of myelination at the promyelinating stage (Bermingham et al., 1996), but extended analysis showed that only a transient stalling of differentiation at this stage actually occurs (Jaegle et al., 1996). During the first postnatal week in large peripheral nerves (e.g., the sciatic nerve), mutant Schwann cells that would normally be destined for myelination are markedly retarded in their development relative to their wild-type counterparts. During subsequent weeks, however, increasingly normal myelination is observed in these mutants, which eventually leads to remarkably robust levels of myelin and nearly normal appearing nerves in young $SCIP^{-/-}$ adults (Jaegle et al., 1996). Interestingly, targeted expression in mouse Schwann cells of a dominant-negative truncation mutant of SCIP (ΔSCIP), using the late-acting myelin-specific promoter of the protein zero (P_0) gene (Lemke et al., 1988; Messing et al., 1992), results in Schwann cell differentiation that is accelerated rather than delayed, such that myelin organelles in these ΔSCIP animals are elaborated days prior to their appearance in wild-type mice (Weinstein et al., 1995).

In contrast to the transient Schwann cell phenotype seen in the SCIP knock-outs, mice homozygous for a loss-of-function Krox-20 mutation exhibit a complete and apparently permanent block in myelinating Schwann cell differentiation at the promyelinating stage, as assessed both morphologically and by dramatically reduced expression of myelin-specific gene products (Murphy et al., 1996; Swiatek and Gridley, 1993; Topilko et al., 1994). Together with the above-mentioned expression data, these observations implicate Krox-20 as a later-acting global regulator of myelination-related gene expression. The peripheral nerves of Krox-20 mutants have also been reported to contain an apparently higher number of Schwann cells relative to wild type, suggesting that this transcription factor may in addition regulate cell cycle exit within the myelinating Schwann cell lineage (Topilko et al., 1994).

The differential expression profiles of SCIP and Krox-20 during the course of late Schwann cell differentiation, together with the differential Schwann cell phenotypes seen in the SCIP and Krox-20 mouse knock-outs, led us to ask whether expression of these two transcription factors is independently regulated during PNS development. More specifically, we ask whether Krox-20 activity is required for the timely downregulation of SCIP expression in the myelinating Schwann cell lineage, by analyzing *Krox-20*$^{-/-}$ sciatic nerves in the second postnatal week (at postnatal day 12), when the vast majority of cells within the myelinating lineage in normal nerves are already actively myelinating and are $SCIP^-$. We observe markedly elevated SCIP expression at postnatal day 12 (P12) in the $Krox\text{-}20^{-/-}$ cells, and a corresponding lack of myelin gene expression, with respect to both protein and RNA. Furthermore, we find that these mutant Schwann cells continue both to proliferate and to be subject to apoptotic cell death at rates even higher than those seen for normal promyelinating cells. In spite of the increased proliferation observed at P12 in the peripheral nerves of Krox-20 mutants, we find that the concomitantly elevated apoptosis is sufficient to maintain a nearly normal number of Schwann cells in these nerves.

MATERIALS AND METHODS

Animal husbandry and genotyping

C57Bl/6 *Krox-20*$^{+/-}$ founder males were crossed into 129SV wild-type females to increase the litter size of subsequent matings by outbreeding. All procedures were carried out in accordance with the Salk Institute guidelines for animal handling. Genomic DNA was extracted from 1 cm sections of mouse tails using standard techniques (Sambrook et al., 1989). Mutant and wild-type Krox-20 alleles were identified by PCR genotyping as previously described (Swiatek and Gridley, 1993).

Immunohistochemistry, BrdU labeling and TUNEL staining

For anti-SCIP and anti-P_0 immunohistochemistry, whole litters of *Krox-20*$^{+/-}$ matings were killed and the sciatic nerves were immersed into 4% paraformaldehyde (PFA) in phosphate-buffered saline (PBS) at 4°C for 2 hours. Subsequently, the nerves were stored separately in 0.1% PFA/PBS at 4°C for several days until genotyping was complete, at which time they were infiltrated in 20% sucrose ON at 4°C before freezing in OCT medium. Otherwise, the cryosectioning was performed as described previously (Zorick et al., 1996).

BrdU injections, anti-SCIP-, anti-P_0- and anti-BrdU-immunohistochemistry were conducted essentially as described previously (Zorick et al., 1996). Donkey anti-mouse and goat anti-rabbit secondary antibodies (conjugated to Cy3 and FITC fluorophores, respectively) were obtained from Jackson ImmunoResearch Laboratories (West Grove, PA) and used as described (Zorick et al., 1996). TUNEL staining to detect DNA fragmentation was performed as described previously (Syroid et al., 1996). All sections were counterstained with bisbenzamide (Zorick et al., 1996).

Quantitative immunohistochemical analyses

All immunolabeled sections were viewed with a Bio-Rad MRC 1024UV confocal scanning laser microscope running Lasersharp software, graciously provided by Dr Fred Gage of the Salk Institute. Adjacent longitudinal sections from pools of several animals of the same genotype were scanned first for bisbenzamide staining and then for either Cy3 or FITC fluorescence. Cy3 and FITC fluorescence scans were done such that only the brightest signals were detected and the confocal settings were kept the same for each immunohistochemical stain, to ensure that the relative signal intensities were recorded accurately, even between different preparations and different genotypes.

Ribonuclease protection analysis

Total cellular RNA was isolated as described previously (Chomczynski and Sacchi, 1987). Ribonuclease protection assays (RPA) were performed using 1 μg total RNA and 10 μg tRNA much as described (Krieg and Melton, 1987), using the Maxiscript in vitro transcription kit (Ambion) from templates containing the following inserts: a 489 bp mouse cyclophilin cDNA fragment (nucleotides 247-736; Hasel and Sutcliffe, 1990), a 260 bp mouse SCIP cDNA fragment (generously provided by John Bermingham, nucleotides 445-705; Suzuki et al., 1990), and a 131 bp mouse P_0 cDNA fragment encompassing 3′-untranslated sequences (nucleotides 429-598 of P_0 exon 5+6 sequence; You et al., 1991). RPA blots were imaged and analyzed using a Molecular Dynamics (Sunnyvale, CA) phosphoimaging device running ImageQuaNT 3.3 software. For densitometry calculation, band intensities for SCIP and P_0 probes were normalized to the band intensity for the cyclophilin control in order to compare relative band intensities between lanes.

Unbiased quantitative stereology

All equipment used for the unbiased stereology was provided by the laboratory of Dr Fred Gage, under the guidance of Dr Dan Peterson. The optical dissector procedure used for unbiased quantitation of cell number has been previously described (Peterson et al., 1994, 1996, 1997). Sciatic nerves from P12 *Krox-20*$^{+/+}$, *Krox-20*$^{+/-}$ and *Krox-20*$^{-/-}$ littermates (from 2 different litters) were fixed in situ for 5 minutes at room temperature (RT) in 4% PFA/PBS. The nerves were then excised 2 mm distal to the sciatic notch, extending distally and postfixed 2 hours at 4°C in 4%PFA/PBS, and subsequently processed for cryosectioning as above. 25 μm cryostat sections were cut as described (Zorick et al., 1996) and collected onto Fisherbrand Superfrost Plus microscope slides (Fisher Scientific, Pittsburgh, PA). Sections were collected, dried ON at RT, immersion fixed in 4% PFA/PBS for 5 minutes at RT, then bisbenzamide stained and mounted in anti-fade mounting media as described (Zorick et al., 1996). After processing, the true thickness of the sections had been reduced to 16 μm, based upon measurement with the computer-driven Z-axis of the stereology stage (data not shown). The relative reference area for each section was calculated by applying a computer-generated grid to the video image of the section, and counting the number of boxes of defined box size (50 μm per side) that overlapped with the nerve.

Quantitative estimates of cell number and volume of sciatic nerve samples from each genotype were made using the optical fractionator principle (West, 1993) and the Cavalieri point count estimator (West and Gundersen, 1990), respectively. Either every sixth serial section (*Krox-20*$^{+/+}$, *Krox-20*$^{+/-}$) or every twelfth serial section (*Krox-20*$^{-/-}$) was examined under appropriate filter sets on an semiautomated stereology system (StereoInvestigator, MicroBrightField, Inc.). Cells were sampled in a 1:16 area subfraction and a 1:1.33 thickness subfraction.

Transfection and luciferase assays

Rat Schwann cells were cultured from neonatal pups, and grown and transfected as described previously (Brown and Lemke, 1997; Zorick et al., 1996) in the presence of recombinant neuregulin-1 (graciously provided by D. Wen of Amgen Corp., Thousand Oaks, CA) and forskolin. Schwann cells in 12-well plates were then transfected with 0.5 μg of 915 bp P_0 promoter-luciferase reporter plasmid (Brown and Lemke, 1997), 0.1 μg of an RSV-β-gal construct to measure transfection efficiency and increasing amounts of a CMV-driven Krox-20 expression vector. CMV vector without Krox-20 cDNA insert was used to keep the total amount of DNA transfected the same for each well. Cells were cultured for 2 days following transfection. Luciferase units were normalized relative to β-gal expression to control for transfection efficiency and data within an experiment were measured as induction by Krox-20 compared to background vector alone.

Sciatic nerve modeling

We are indebted to Dr Mike DeWeese of the Sejnowski laboratory at the Salk Institute for mathematical advice. To model the fraction of cells undergoing cell death during postnatal development as a function of time, we used a sigmoid function with fitted constants to fit the experimental data and assumptions made (see Results) using MathCad 7 professional software (MathSoft, Inc.). Numerical integration of Schwann cell growth with and without death was performed using the same program. Numerical data from these calculations was imported into Microcal Origin 4.1 (Microcal, Inc.) to graph, and the graphs subsequently modified using Canvas 3.5 and 5.0 (Deneba Systems, Inc.).

RESULTS

SCIP expression is maintained in postnatal *Krox-20*$^{-/-}$ Schwann cells

During the normal development of rodent sciatic nerves, the percentage of SCIP$^+$ Schwann cells declines from a peak near the day of birth to less than 1% by P13 in the rat (~P11 in the mouse), while the percentage of Krox-20$^+$ cells rises during the first two postnatal days and is stable thereafter (Zorick et al., 1996). Using *Krox-20*$^{-/-}$ mice, we asked whether the pronounced downregulation of SCIP in the myelinating lineage is dependent upon Krox-20. We decided to closely examine the P3 and P12 time points, since at P3 most sciatic nerve Schwann cells destined for myelination are still SCIP$^+$, many are capable of cell division and only a few are actively myelinating; whereas at P12, nearly all of these cells are SCIP$^-$, most are actively myelinating, and very few are dividing. In addition, the high mortality rate of *Krox-20*$^{-/-}$ mice at birth and their short life span thereafter made P12 the latest practical time at which we were routinely able to obtain homozygous knockouts for analysis (Schneider-Maunoury et al., 1993; Swiatek and Gridley, 1993).

Using a specific, high-affinity SCIP antibody (Zorick et al., 1996), we examined P12 *Krox-20*$^{-/-}$ sciatic nerves, along with those of heterozygous and wild-type littermates, for SCIP immunoreactivity (Fig. 1A). We observed SCIP expression in the majority of P12 *Krox-20*$^{-/-}$ Schwann cell nuclei, compared to the rare SCIP$^+$ nuclei that were detectable in the P12 nerves of control (*Krox-20*$^{+/-}$ and *Krox-20*$^{+/+}$) littermates. Since previous reports indicated that *Krox-20*$^{-/-}$ sciatic nerves contain a higher density of Schwann cells than unaffected littermates (Topilko et al., 1994), observed increases in the incidence of SCIP immunoreactivity might in part reflect this increased density. We therefore quantitated the proportion of SCIP$^+$ cells at P3 and P12, in *Krox-20*$^{-/-}$, *Krox-20*$^{+/-}$ and *Krox-20*$^{+/+}$ sciatic nerves, by comparing SCIP expression to the total

number of nuclei as visualized by bisbenzamide staining (Fig. 1B). We found that 52% of Schwann cells were intensely SCIP$^+$ at P12 in *Krox-20*$^{-/-}$ sciatic nerves, whereas only 2% and 1% still strongly expressed this transcription factor at P12 in heterozygous and wild-types nerves, respectively. Interestingly, the percentage of SCIP$^+$ cells visualized with the antibody at P12 in the homozygous Krox-20 knockouts was very similar to the percentage observed at P3 for all genotypes (Fig. 1B). We further found that the failure of *Krox-20*$^{-/-}$ Schwann cells to downregulate SCIP at P12 was accompanied by a corresponding failure to upregulate expression of the *P0* gene, whose high level expression is normally tied to the onset of overt myelination (Fig. 1A,C). Antibody expression data (Fig. 1A,B) were complemented by ribonuclease protection assay, using probes specific for SCIP, P_0 and the ubiquitous cellular marker cyclophilin (Fig. 1C). These data demonstrate that the increased SCIP expression and reduced P_0 expression of P12 *Krox-20*$^{-/-}$ sciatic nerves is effected at the RNA level. Densitometry revealed that P_0 mRNA levels were decreased ~15-fold and SCIP mRNA levels increased ~6 fold in P12 *Krox-20*$^{-/-}$ sciatic nerves as compared to wild-type and heterozygous littermates (Fig. 1C; data not shown). These observations demonstrate that Krox-20 activity is essential for the timely extinguishing of SCIP expression in the myelinating Schwann cell lineage, and that SCIP and Krox-20 are not regulated independently. They further demonstrate that, in the absence of Krox-20, SCIP is not able to downregulate its own expression.

Krox-20$^{-/-}$ Schwann cells do not withdraw from the cell cycle

The control of Schwann cell proliferation during peripheral nerve development has been the subject of several previous studies (Brown and Asbury, 1981; Friede and Samorajski, 1968; Martin and Webster, 1973; Stewart et al., 1993; Webster et al., 1973). In particular, it has been shown that Schwann cell mitotic activity in the mouse peaks during late embryogenesis and declines thereafter, such that by the second postnatal week very little cell division can be detected in major peripheral nerves (Friede and Samorajski, 1968; Stewart et al., 1993). We asked whether this progressive loss of cell division, which is concomitant with the onset of myelination, is also dependent on Krox-20 activity. We performed short BrdU pulse-labelings in vivo, followed by immunohistochemical detection of BrdU$^+$ nuclei, to acutely label *Krox-20*$^{-/-}$ Schwann cells in the S phase of the cell cycle, relative to *Krox-20*$^{+/-}$ and *Krox-20*$^{+/+}$ littermates (Fig. 2A). We again focused on P3 and P12, for the reasons outlined above. We found that, while P3 *Krox-20*$^{-/-}$ sciatic nerves do not exhibit any significant differences in the pattern or apparent fraction of mitotic cells relative to control nerves, P12 *Krox-20*$^{-/-}$ nerves contain many more Schwann cells that are undergoing DNA synthesis than do nerves from control littermates (Fig. 2A). We measured this fraction by double labeling with bisbenzamide, and performed appropriate statistical comparisons between cells of each genotype at P3 and P12 (Fig. 2B). Fig. 2 demonstrates that the fraction of Schwann cells in the mitotic cycle in P12 *Krox-20*$^{-/-}$ mice is increased more than 5-fold relative to heterozygous and wild-

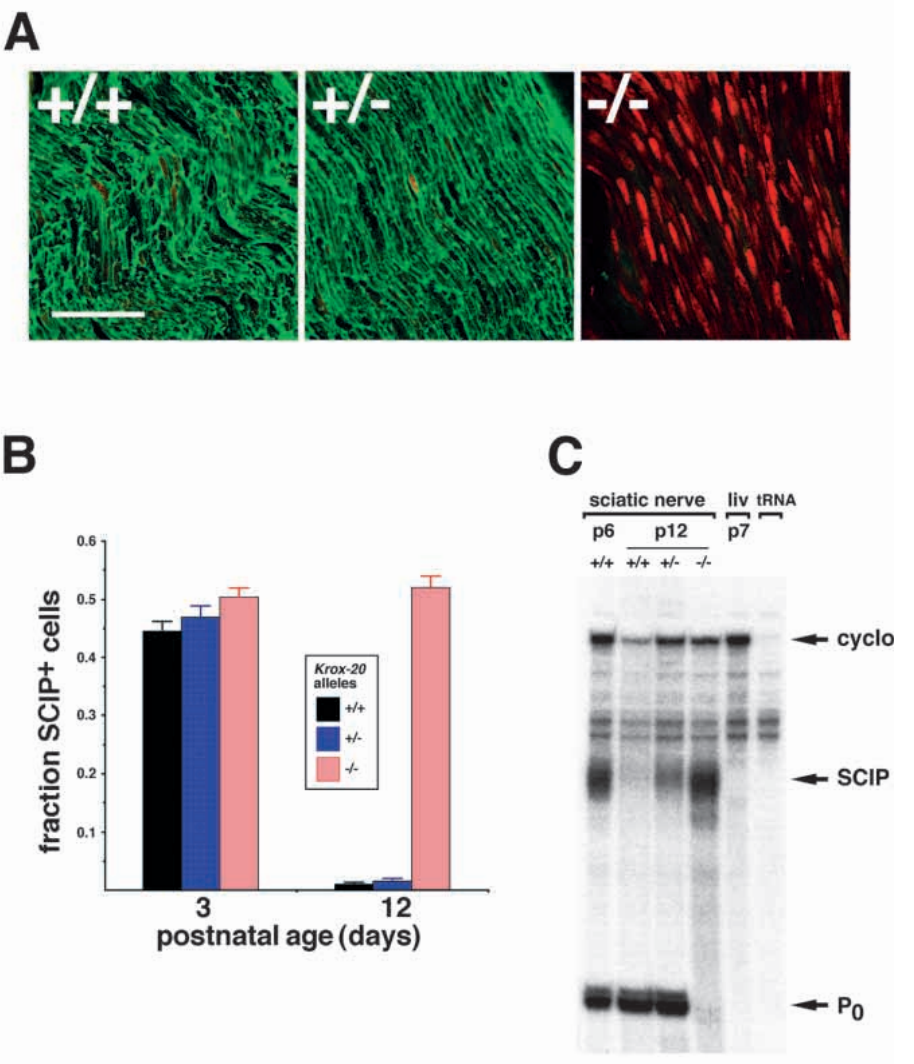

Fig. 1. SCIP expression in wild-type and Krox-20 mutant sciatic nerves. (A) Longitudinal sections of P12 *Krox-20*$^{+/+}$, *Krox-20*$^{+/-}$ and *Krox-20*$^{-/-}$ sciatic nerves, double immunolabeled for SCIP (red) and P_0 glycoprotein (green). Bar represents 50 μm. (B) Quantitative analysis of SCIP expression in P3 and P12 *Krox-20*$^{+/+}$, *Krox-20*$^{+/-}$ and *Krox-20*$^{-/-}$ sciatic nerves. Data represent the fraction of nuclei labeled with bisbenzamide that also strongly express SCIP. Note that the same confocal settings were used throughout the experiment. Data are presented as the mean±sep. For P3: +/+, n=727; +/–, n=551; –/–, n=913. For P12: +/+, n=694; +/–, n=603; –/–, n=805, P<0.001 by chi-squared analysis. (C) Ribonuclease protection assay of sciatic nerve RNA from P12 animals of Krox-20$^{+/+}$, *Krox-20*$^{+/-}$ and *Krox-20*$^{-/-}$ genotypes, compared to a wild-type P6 control sciatic nerve and a P7 liver, hybridized with probes to SCIP, cyclophilin and P_0 RNA.

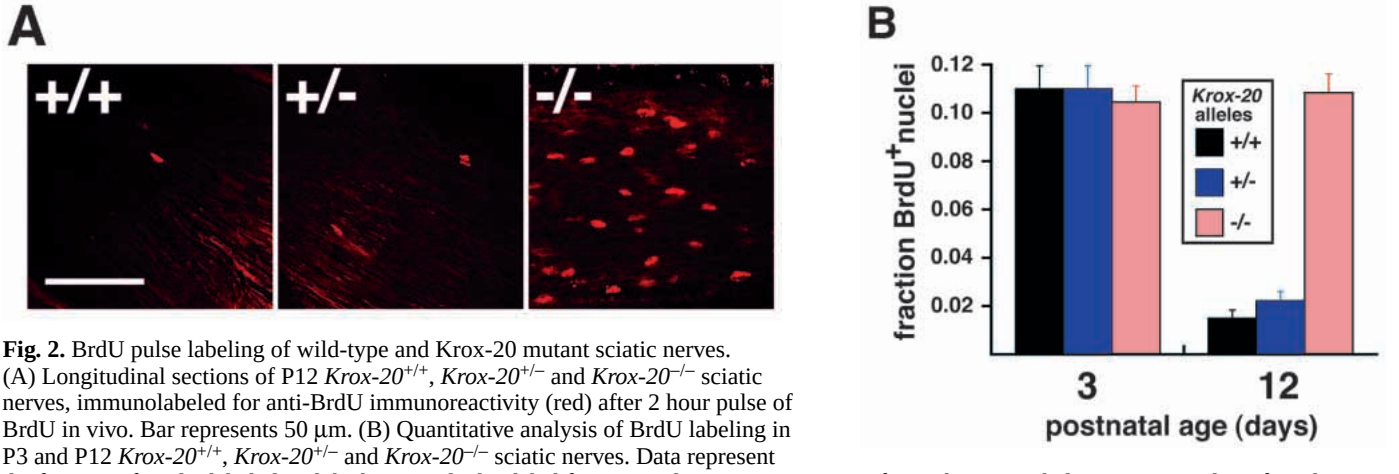

Fig. 2. BrdU pulse labeling of wild-type and Krox-20 mutant sciatic nerves. (A) Longitudinal sections of P12 *Krox-20*$^{+/+}$, *Krox-20*$^{+/-}$ and *Krox-20*$^{-/-}$ sciatic nerves, immunolabeled for anti-BrdU immunoreactivity (red) after 2 hour pulse of BrdU in vivo. Bar represents 50 μm. (B) Quantitative analysis of BrdU labeling in P3 and P12 *Krox-20*$^{+/+}$, *Krox-20*$^{+/-}$ and *Krox-20*$^{-/-}$ sciatic nerves. Data represent the fraction of nuclei labeled with bisbenzamide that label for anti-BrdU immunoreactivity for each time. Labeling was carried out for 2 hours at P12 to ensure an accurate estimate of the very low number of +/+ and +/– Schwann cells still capable of dividing at this time. Data are presented as the mean±sep. For P3: +/+, n=1328; +/–, n=1226; –/–, n=1782. For P12: +/+, n=1565; +/–, n=1069; –/–, n=1521, P<0.001 by chi-squared analysis.

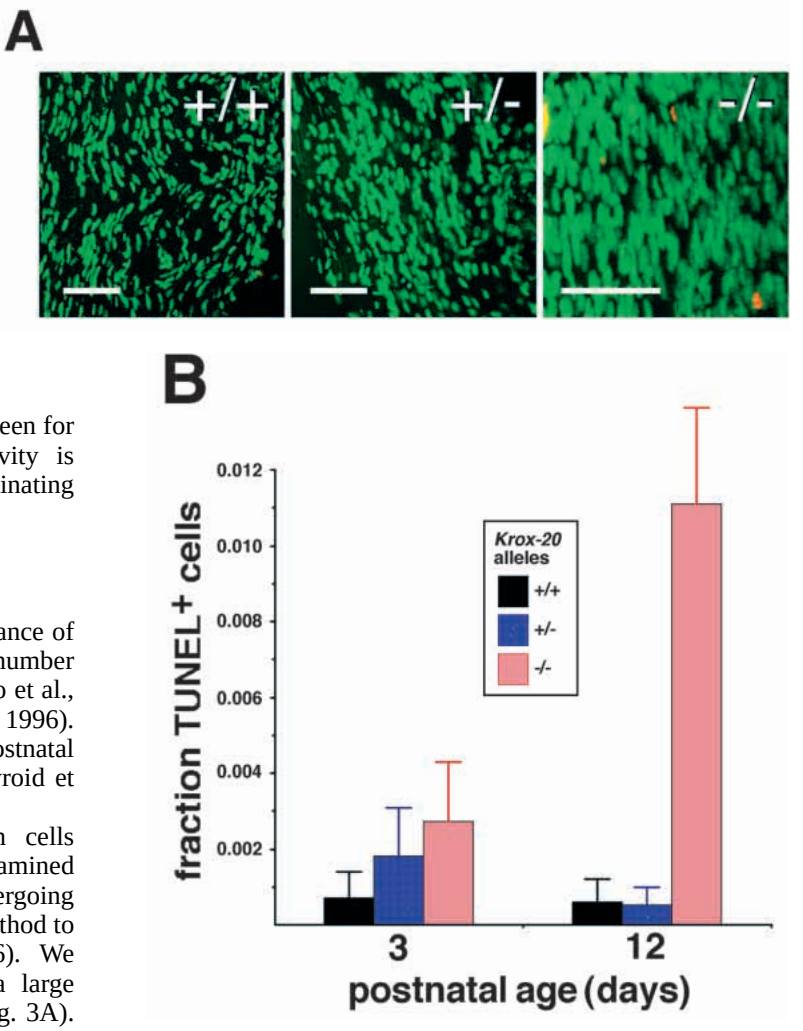

Fig. 3. TUNEL labeling of wild-type and Krox-20 mutant sciatic nerves. (A) Longitudinal sections of P12 *Krox-20*$^{+/+}$, *Krox-20*$^{+/-}$ and *Krox-20*$^{-/-}$ sciatic nerves, labeled for DNA fragmentation by TUNEL staining (red) and bisbenzamide (green). Bars represent 50 μm. (B) Quantitative analysis of TUNEL labeling in P3 and P12 *Krox-20*$^{+/+}$, *Krox-20*$^{+/-}$ and *Krox-20*$^{-/-}$ sciatic nerves. Data represent the fraction of nuclei labeled with bisbenzamide that label for TUNEL stain for each time. Note that the same confocal settings were used throughout the experiment. Data are presented as the mean±sep. For P3: +/+, n=1337; +/–, n=1135; –/–, n=1100. For P12: +/+, n=1714; +/–, n=1930; –/–, n=1798, P<0.001 by chi-squared analysis.

type littermates and is approximately the same as that seen for P3 Schwann cells of all genotypes. Krox-20 activity is therefore required for the normal withdrawal of myelinating Schwann cells from the cell cycle.

Krox-20$^{-/-}$ Schwann cells exhibit dramatically increased apoptosis at P12

Recently, we and others have demonstrated the importance of apoptosis as a mechanism to regulate Schwann cell number during PNS development (Grinspan et al., 1996; Nakao et al., 1997; Syroid et al., 1996; Trachtenberg and Thompson, 1996). Schwann cell apoptosis is evident during the first two postnatal weeks and declines thereafter (Nakao et al., 1997; Syroid et al., 1996).

Based on our finding that *Krox-20*$^{-/-}$ Schwann cells proliferate abnormally within peripheral nerves, we examined *Krox-20*$^{-/-}$ sciatic nerves for the number of cells undergoing apoptosis, using the TUNEL histochemical staining method to visualize DNA fragmentation (Syroid et al., 1996). We observed that P12 *Krox-20*$^{-/-}$ sciatic nerves have a large apparent increase in the number of TUNEL^{+} cells (Fig. 3A). We quantitated this increase by determining the fraction of Schwann cells positive for the TUNEL stain at a given age, to account for differences in cell density seen between genotypes (Fig. 3B). At P3, *Krox-20*$^{-/-}$ Schwann cells exhibit no statistically significant difference in the level of apoptosis as compared to heterozygous and wild-type littermates (although a non-significant trend is evident). Moreover, the amount of

apoptotic activity that we observed in mice at this time is essentially the same as that previously reported for the rat (Fig. 3B; Syroid et al., 1996). However, by P12, a point at which wild-type and *Krox-20*$^{+/-}$ sciatic nerves each exhibit a very slightly reduced level of apoptotic activity relative to P3, the *Krox-20*$^{-/-}$ Schwann cell population is subject to exceptionally high levels of programmed cell death: these cells undergo apoptosis at a rate that is 16-fold higher than their wild-type counterparts at P12, and more than 5-fold higher than even mutant cells at P3.

Krox-20 transactivates the P_0 promoter in co-transfection experiments

The loss of Krox-20 activity results in an apparent block to Schwann cell differentiation at the promyelinating-to-myelinating transition and a marked reduction in the level of myelin-specific gene expression, as exemplified by P_0 expression (Fig. 1A,C; Topilko et al., 1994). This observation, together with the fact that Krox-20 is expressed throughout myelination and into adulthood, has suggested that Krox-20 acts as a positive regulator of myelin gene expression (Zorick et al., 1996). To address this possibility, we conducted transient transfection experiments using purified and cultured rat Schwann cells (Monuki et al., 1990, 1993). A CMV-driven Krox-20 expression plasmid and a reporter plasmid containing 915 bp of 5′ flanking DNA from the P_0 promoter linked to a luciferase reporter gene (Brown and Lemke, 1997; Lemke et al., 1988) were cotransfected at varying concentrations into rat Schwann cells grown in the presence of forskolin. These cells were incubated for 2 days and then assayed for luciferase activity. A representative experiment is shown in Fig. 4. Even in the face of endogenous Schwann cell expression of Krox-20 (Zorick et al., 1996), we observed that transfected Krox-20 is capable of a 2-fold transactivation of the cloned P_0 promoter with as little as 50 ng transfected Krox-20 expression plasmid, and that roughly 4-fold transactivation is possible with higher levels of this plasmid. Although these data do not address the issue of whether Krox-20 binds to the P_0 regulatory region, they do demonstrate that this transcription factor is, either directly or indirectly, capable of transactivating through a set of DNA regulatory elements that are only active in myelinating Schwann cells. This observation supports the hypothesis that Krox-20 serves as a global transactivator of myelin gene expression in the Schwann cell lineage.

Total Schwann cell number is relatively conserved in *Krox-20*$^{-/-}$ sciatic nerves

Given our surprising results with regard to elevated mitotic activity and apoptosis in Krox-20-deficient Schwann cells, we became interested in the control of total cell number within the myelinating lineage. The initial description of the peripheral nerve phenotype of *Krox-20*$^{-/-}$ mutant mice reported a higher density of Schwann cells at P15 as compared to wild-type littermates (Topilko et al., 1994). However, measurements of cell density are highly susceptible to processing-based errors caused by shrinkage artifacts, resulting in quantitative errors (for discussions, see Peterson et al., 1994, 1996, 1997). We therefore employed unbiased quantitative stereology on cross sections of P12 *Krox-20*$^{-/-}$, *Krox-20*$^{+/-}$ and wild-type sciatic nerves to accurately estimate the number of cells in a defined length of nerve, in addition to the cellular density (Peterson et al., 1997). The results are illustrated in Table 1. In agreement with Topilko et al. (1994), we find that the cellular density of late postnatal *Krox-20*$^{-/-}$ sciatic nerves is indeed increased, by roughly 3-fold compared to heterozygous and wild-type littermates, with a concomitant 4-fold decrease in the average cross-sectional area (Table 1). However, the measured total cell number of a 300 μm length of P12 Krox-20-deficient sciatic nerve was only ~45% higher than the corresponding number for wild-type and heterozygous littermates. Apoptosis is therefore apparently able to compensate for the increased proliferation present throughout postnatal development.

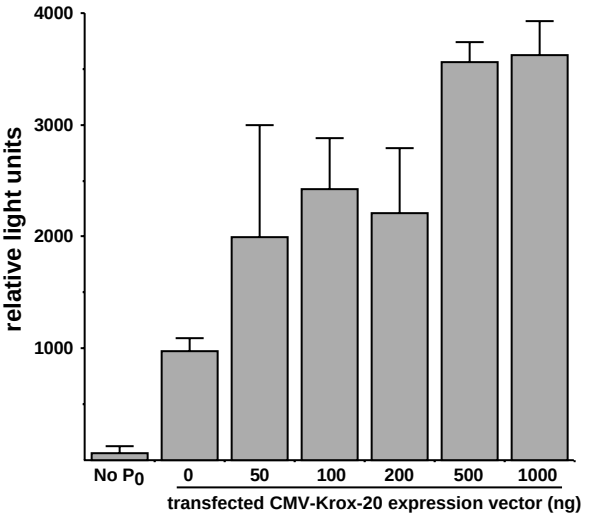

Fig. 4. Cultured rat Schwann cells were transfected with 0.5 μg of a luciferase plasmid in which reporter gene expression is driven by 915 bp of 5′ flanking DNA from the rat P_0 gene (Lemke et al., 1988), together with increasing amounts of a CMV-Krox-20 plasmid, or with the empty CMV vector alone. Data are shown as mean±s.e.m. *n*=4.

Models of Schwann cell proliferation

Given these observations, we decided to model Schwann cell population dynamics within the sciatic nerves of both wild-type and *Krox-20*$^{-/-}$ mice (Fig. 5). First, we used a formula proposed by Brown and Asbury (1981) for estimating the fraction of Schwann cells in the mitotic cycle as a function of postnatal age in wild-type mice: y=1/(2+x), where y=fraction of dividing Schwann cells, and x=postnatal day. We integrated this equation over the first two weeks of postnatal life, given the previously published estimate for Schwann cell cycle duration of 1 day (see Stewart et al., 1993 for a discussion). In

Table 1. Unbiased quantitative stereology on P12 *Krox-20*$^{-/-}$, *Krox-20*$^{+/-}$ and *Krox-20*$^{+/+}$ sciatic nerves

Krox-20 allele	Vref (μm^3)	Nfv	Total cells (Nabs)	Cell density (cells/μm^3)
+/+	1.55E+08	358	4.55E+04	2.9E–04
+/–	1.56E+08	349	4.47E+04	2.9E–04
–/–	4.33E+07	502	6.50E+04	1.0E–03

Calculated total reference volume (Vref), number of cells counted per fractional volume (Nfv), calculated total cells (Nabs) and calculated cell density are reported, based upon measurements taken by the optical dissector method for each genotype (Peterson et al., 1997).

the absence of cell death, these parameters yield a Schwann cell population that increases linearly with time (upper curve, Fig. 5A), but with a rate of increase that exceeds estimates derived from experimental data (Nakao et al., 1997; Peters and Muir, 1958). We therefore added an estimate of apoptotic death before integration, by setting the steady-state percentage of apoptotic cells throughout the first two postnatal weeks at a constant 0.18%, in accordance with our previous measurements (Syroid et al., 1996). To calculate the fraction of cells lost per day, we estimated that apoptotic Schwann cells might have a clearance time ranging anywhere from 30 minutes to 6 hours, based on measurements of the clearance time for apoptotic oligodendrocytes in the developing optic nerve (Barres et al., 1992; Barres and Raff, 1994), and for newly born embryonic neurons (Thomaidou et al., 1997). By integrating these varying estimates of apoptotic cell loss (normalized to day length) with the formula for cell growth, we derived the lower curves in Fig. 5A. The curve generated using a 1 hour clearance time most closely approximates the experimentally determined dynamics of the postnatal Schwann cell population within wild-type peripheral nerves (Nakao et al., 1997; Peters and Muir, 1958).

Next, we asked whether our experimentally derived data for proliferation, apoptosis and Schwann cell number in *Krox-20*$^{-/-}$ sciatic nerves could, if incorporated into the above modeling equation, account for the fact that the dramatically different proliferative and apoptotic rates observed in *Krox-20*$^{-/-}$ mutant nerves result in only a modest (~45%) increase in cell number relative to wild type. To facilitate this analysis, we made additional measurements of cell death at P7 in *Krox-20*$^{-/-}$ nerves (Table 2). Based on earlier observations, we assumed that: (a) the apoptotic rates at P0 and P3 in the *Krox-20* mutants were identical to that for wild type and mutants at P3 and (b) the *Krox-20*$^{-/-}$ apoptotic rate between P12 and P15 was constant at the rate measured for P12. These parameters were used to fit a sigmoid curve that describes the incidence of apoptotic cell death occurring in *Krox-20*$^{-/-}$ Schwann cells as a function of postnatal age (Fig. 5B). We also used a constant value of 25% for the fraction of *Krox-20*$^{-/-}$ Schwann cells in mitosis between P3 and P12 (Fig. 2B), which is similar to that previously reported for P2/3 wild-type cells (Brown and Asbury, 1981; Friede and Samorajski, 1968; Nakao et al., 1997). Our measured fraction of cells pulse-labeled at P3 with BrdU in the mouse (Fig. 2) is approximately 3-fold lower than this percentage because the S phase of the cell cycle is approximately 8 hours long, as compared to the 24-hour-long cell cycle (Stewart et al., 1993). This 3-fold conversion factor normalizes our experimental data to the fraction of cells in mitosis per day.

Given (a) this cell density estimate, (b) the equation that we derived that models the change in the rate of apoptosis in the Krox-20 mutants over the same period (Fig. 5B), and (c) the assumption that the lack of Krox-20 activity did not affect either the cell cycle length (24 hours) or clearance time of apoptotic cells, we then performed a series of numerical integrations (Fig. 5C). Without allowance for apoptosis, a constant 25% proliferation rate would quickly result in a severely hypertrophic sciatic nerve in the mutant (Fig. 5A,C, upper curves). When the derived equations for apoptotic rate change in the mutants are added to the integration, only in the case of the 1 hour clearance time does the resulting cell number approach a stabilized level by P12 (Fig. 5C, lower curve). Remarkably, when the modeled curve for wild-type growth with apoptosis is compared directly to the modeled *Krox-20*$^{-/-}$ curve with apoptosis with the 1 hour clearance time, it can be seen that the mutant sciatic nerve is predicted to exhibit a ~40% increase in Schwann cell number relative to wild type at P12 (Fig. 5D). Although this modeling relies on interpolations, it is in exceptionally close agreement with the observed value of ~45% (Table 1).

Table 2. Summary of data and assumptions used to model the change in apoptosis over time in *Krox-20*$^{-/-}$ sciatic nerves

Timepoint (postnatal day)	Apoptotic nuclei (%)	Source
0	0.2	assumption
3	0.2	experiment
7	0.7	experiment
12	1.1	experiment
15	1.1	assumption
20	1.1	assumption

Following the reasoning described in the text, estimates for the percentage of apoptotic nuclei at a given time for P3, P7 and P12 are derived from experimental data in this work. For P0, we assume that the fraction of apoptotic nuclei is essentially the same as reported previously in the rat for the average fraction over the first postnatal week (Syroid et al., 1996). For P15 and P20, we assume that the fraction of apoptotic nuclei is essentially the same as experimentally determined for P12, which provides for a stable Schwann cell population in the sciatic nerve given the experimentally determined estimate of cell proliferation and apoptotic clearance time (see Results).

DISCUSSION

SCIP as a transitional regulator

Our results demonstrate that the striking downregulation of SCIP expression that normally follows the onset of myelination is completely dependent on Krox-20 and that, in the absence of this transcription factor, SCIP is incapable of autoregulation (self downregulation). We therefore predict that any transgenic manipulation that results in the aberrant maintenance of a promyelinating Schwann cell morphology – even one not directly related to a transcription factor, such as the overexpression or mutation of a myelin structural protein (see for example Adlkofer et al., 1995; Sereda et al., 1996) – will lead to a cell that continues to express SCIP. The fact that SCIP and Krox-20 are not independently regulated, together with the observation that the Krox-20 and SCIP mouse knock-outs exhibit obvious differences in the severity and permanence of Schwann cell dysmyelination, provides the basis for a clearer appreciation of the distinct roles that these two proteins play during myelination.

Since apparently all *SCIP*$^{-/-}$ Schwann cells that would normally be destined to myelinate eventually do so if given adequate developmental time (Jaegle et al., 1996), SCIP is not an essential forward driver of the promyelinating-to-myelinating transition. Rather, we propose that this transcription factor provides a mechanism through which Schwann cells smoothly transit between markedly different states of gene expression and cellular phenotype, by transiently binding to and thereby disabling a subset of the cell's

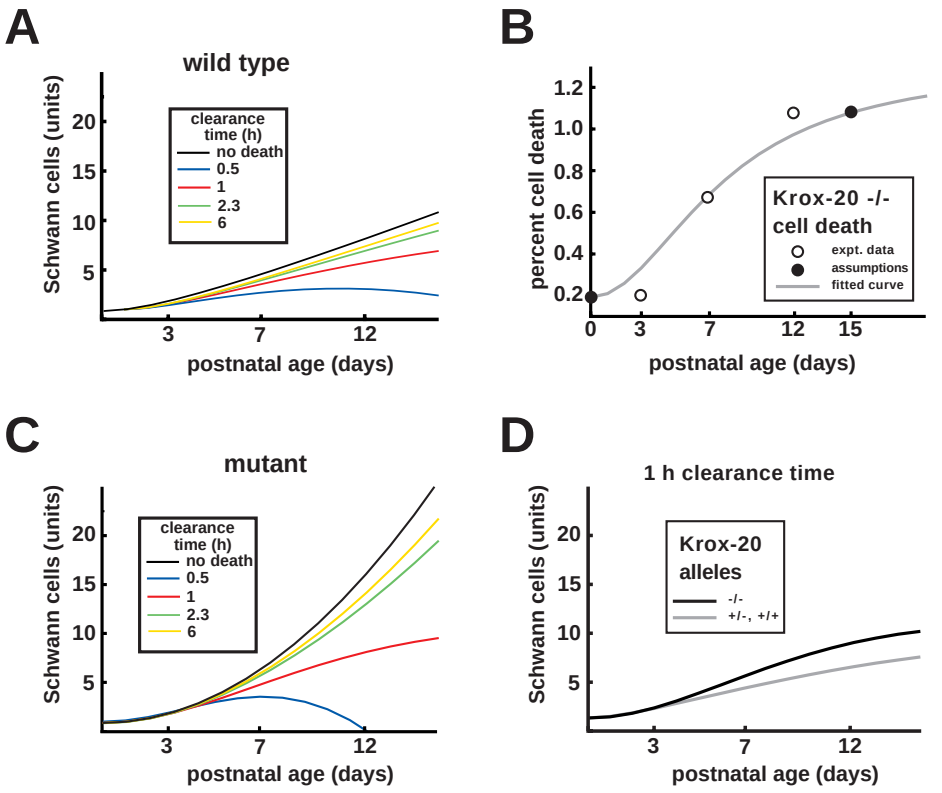

Fig. 5. Models of the postnatal growth kinetics of sciatic nerve Schwann cells. (A) Model of the growth kinetics of *Krox-20*$^{+/+}$ and *Krox-20*$^{+/-}$ sciatic nerve Schwann cells, using the equation y=1/2+x, with and without the estimates of cell death and varying clearance times for apoptotic nuclei, as detailed in the text. Y axis units (cell number) are arbitrary, assuming a starting point of 1 at postnatal day 0. (B) Curve fitting for the change in the incidence of Schwann cell apoptosis occurring in the sciatic nerve as a function of time during postnatal development. Using MathCad software, a sigmoidal curve was generated to best fit the data as presented in Table 2. The best fit curve has the formula $y=(0.477x^{2)}/(100.4+1.6x^{2})$. (C) Model of the growth kinetics of *Krox-20*$^{-/-}$ sciatic nerve Schwann cells, with and without the sigmoidal estimate of cell death, and varying clearance times for apoptotic nuclei, as derived in 5B. (D) Overlay of wild-type and Krox-20$^{-/-}$ curves with an estimated 1 hour clearance time from A and C, respectively, on the same graph.

transcriptional apparatus. We envision that SCIP could play this role through the demonstrated ability of its POU domain to interact with non-histone chromatin proteins such as HMG-I/Y, and with other nuclear scaffolding proteins (Herr and Cleary, 1995; Leger et al., 1995) and thereby disable transcription. In this respect, SCIP function would be analogous to that of a clutch pedal in an automobile transmission: in order to smoothly change from the expression of early genes not related to myelination, such as the *p75* gene, to late genes required for myelination, such as the *P*$_0$ gene, i.e., to smoothly shift developmental ‘gears’, SCIP expression would first be activated and then subsequently deactivated during Schwann cell differentiation just as an automobile clutch pedal is first depressed and then subsequently released in moving from one gear to another. Such a mode of action would allow for the timely and coordinated assembly of transcription factors, such as Krox-20, which are essential for activation of end-stage myelination genes, and would prevent the premature expression of these genes in the same way that an automobile’s engine does not yet drive a selected gear when the clutch pedal is depressed.

This hypothesis has several appealing features with regard to the interpretation of previously puzzling aspects of SCIP and Krox-20 expression, activity and mutant phenotypes. First, it accounts for all of the observed mutant phenotypes. *SCIP*$^{-/-}$ Schwann cells have difficulty entering the myelinating phase, but are not permanently blocked in their forward differentiation, just as it is possible to change automobile gears without a clutch pedal – given sufficient effort, time and grinding of the transmission. *P*$_0$*-ΔSCIP* Schwann cells, on the other hand, differentiate prematurely because the dominant-negative SCIP antagonist in these mice is activated by the P$_0$ promoter only after the cells have already entered the promyelinating phase, just as prematurely releasing (‘popping’) the clutch pedal forces an automobile to lurch into the selected gear. And *Krox-20*$^{-/-}$ Schwann cells are permanently dysmyelinating because this transcription factor acts as a forward gear to drive differentiation. Second, the hypothesis that SCIP disables transcription factors that drive differentiation is consistent with both its transient expression in normal development (Monuki et al., 1989, 1990) and with its transient re-appearance when Schwann cells reverse course and de-differentiate following nerve injury (Monuki et al., 1990; Scherer et al., 1994; Zorick et al., 1996). Third, this hypothesis accounts for the observation that SCIP acts as an exceptionally potent repressor of myelin gene expression when analyzed in cultured Schwann cells (Monuki et al., 1990, 1993). Co-transfected SCIP expression constructs strongly repress transcription of reporter constructs that are linked to myelin (P$_0$ or myelin basic protein) gene promoters, and are, on a molar basis, approximately 10-fold more potent as repressors of these constructs than they are as activators of octamer-driven reporters. Again, this repressor activity can be envisioned to result from POU-domain-dependent binding to nuclear scaffolding proteins and can be analogized to the ‘repressor activity’ exerted over the gears of an automobile transmission when the clutch pedal is depressed. In principal, this model is not substantially different from other recently proposed theories for SCIP function, including the suggestion that SCIP acts as a so-called ‘competence factor’ for myelination (Jaegle and Meijer, 1998).

Both transient expression and repressor activity against end-stage differentiation genes are also exhibited by SCIP during the development of mammalian keratinocytes (Faus et al.,

1994). Furthermore, transient expression of SCIP and other POU domain genes during both neural and non-neural development is the rule rather than the exception (e.g., Collarini et al., 1992; Schreiber et al., 1997; Frantz et al., 1994). Expression of the POU proteins miti-mere and pdm2 during the development of the *Drosophila* neuroblast 4-2 lineage, for example, is strikingly similar – with regard to onset, timing and transience – to that of SCIP in the mammalian Schwann cell lineage, and the neuronal differentiation phenotypes of loss-of-function and dominant-negative mutations in these *Drosophila* genes closely parallel those seen for SCIP in Schwann cells (Bhat et al., 1995; Bhat and Schedl, 1994).

Transcriptional control of Schwann cell number

The results presented above illustrate that loss of an essential forward gear for Schwann cell differentiation, the transcription factor Krox-20, results in aberrations in both cell cycle regulation and the apoptotic control of cell number. In terms of SCIP expression, morphology (Topilko et al., 1994) and proliferation rate, *Krox-20*$^{-/-}$ Schwann cells appear locked into a promyelinating differentiation state. Overall, the Schwann cell population of Krox-20-deficient peripheral nerves in the second postnatal week is exceptionally dynamic, despite approaching steady-state in terms of cell number: this population remains SCIP^{+}, proliferative, apoptotic and non-myelinating at a time when the Schwann cells of normal nerves are SCIP^{-}, quiescent and actively myelinating.

Since SCIP expression is normally activated near the end of the proliferative period for developing Schwann cells and since POU proteins have been demonstrated to promote cell division in other circumstances, it is possible that the maintained SCIP expression in *Krox-20*$^{-/-}$ Schwann cells itself drives their continued proliferation. The fact that these cells also exhibit an extraordinary increase in the rate of cell death during the second postnatal week – more than five times greater than that seen at P3 – may be a downstream consequence of increased Schwann cell competition for limiting amounts of axon-supplied survival factors. Among the several candidates that have been implicated as trophic factors for developing Schwann cells, the case is strongest for neuregulin-1 (NRG-1; Grinspan et al., 1996; Syroid et al., 1996; Trachtenberg and Thompson, 1996), a neuronal, axon-displayed product whose levels in a given peripheral nerve are thought to be determined at least in part by the number of axons that the nerve contains. This growth factor has been shown to rescue Schwann cells from programmed cell death in a variety of experimental settings. If the supply of NRG-1 is truly limiting and if Schwann cells depend on axonal contact for survival, then continued proliferation would directly lead to elevated apoptosis. It should be noted that maintained SCIP expression is by itself unlikely to cause apoptosis, since Schwann cells cultured in the presence of cAMP-elevating agents and NRG-1 are strongly SCIP^{+}, but are not apoptotic (Syroid et al., 1996).

The compound phenotypes of Krox-20 and SCIP mutant Schwann cells, and the differential yet dependent regulation of SCIP and Krox-20 in developing peripheral nerves, together demonstrate that these transcription factors exert distinct activities at different points in Schwann cell differentiation. While the initial activation of SCIP function in Schwann cells appears to be important for entry into the promyelinating phase, the subsequent extinguishing of SCIP function appears to be essential for exiting this phase. In the absence of promyelinating phase activation of Krox-20, SCIP downregulation never occurs and Schwann cells are arrested in their differentiation. We anticipate that the developmental expression and activity of other transcriptional regulators of myelination will prove to be equally dynamic.

We thank Patrick Burrola, Danny Ortuño and Darcie Baynes for excellent technical assistance, Mike DeWeese and Charles Stevens for advice on modeling, and Dan Peterson and Rusty Gage of the Salk Institute Gene Expression Laboratory for technical assistance, use of confocal and stereology microscopy equipment, and advice on experimental design. This work was supported by predoctoral fellowships from the Department of Defense and the NIH (T. S. Z.), by postdoctoral fellowships from the National Multiple Sclerosis Society (D. E. S. and A. B.) and the Muscular Dystrophy Association (A. B.), and by grants from the NIH (G. L.).

REFERENCES

Adlkofer, K., Martini, R., Aguzzi, A., Zielasek, J., Toyka, K. V. and Suter, U. (1995). Hypermyelination and demyelinating peripheral neuropathy in Pmp22-deficient mice. *Nat. Genet.* **11**, 274-280.

Barres, B. A., Hart, I. K., Coles, H. S., Burne, J. F., Voyvodic, J. T., Richardson, W. D. and Raff, M. C. (1992). Cell death and control of cell survival in the oligodendrocyte lineage. *Cell* **70**, 31-46.

Barres, B. A. and Raff, M. C. (1994). Control of oligodendrocyte number in the developing rat optic nerve. *Neuron* **12**, 935-942.

Bermingham, J. R. j., Scherer, S. S., O'Connell, S., Arroyo, E., Kalla, K. A., Powell, F. L. and Rosenfeld, M. G. (1996). Tst-1/Oct-6/SCIP regulates a unique step in peripheral myelination and is required for normal respiration. *Genes Dev.* **10**, 1751-1762.

Bhat, K. M., Poole, S. J. and Schedl, P. (1995). The miti-mere and pdm1 genes collaborate during specification of the RP2/sib lineage in Drosophila neurogenesis. *Mol. Cell. Biol.* **15**, 4052-4063.

Bhat, K. M. and Schedl, P. (1994). The Drosophila miti-mere gene, a member of the POU family, is required for the specification of the RP2/sibling lineage during neurogenesis. *Development* **120**, 1483-1501.

Blanchard, A. D., Sinanan, A., Parmantier, E., Zwart, R., Broos, L., Meijer, D., Meier, C., Jessen, K. R. and Mirsky, R. (1996). Oct-6 (SCIP/Tst-1) is expressed in Schwann cell precursors, embryonic Schwann cells, and postnatal myelinating Schwann cells: comparison with Oct-1, Krox-20, and Pax-3. *J. Neurosci. Res.* **46**, 630-640.

Brown, A. and Lemke, G. (1997). Multiple regulatory elements control transcription of the peripheral myelin protein zero gene. *J. Biol. Chem.* **272**, 28939-28947.

Brown, M. J. and Asbury, A. K. (1981). Schwann cell proliferation in the postnatal mouse: timing and topography. *Exp. Neurol.* **74**, 170-186.

Chomczynski, P. and Sacchi, N. (1987). Single-step method of RNA isolation by acid guanidinium thiocyanate-phenol-chloroform extraction. *Anal. Biochem.* **162**, 156-159.

Collarini, E. J., Kuhn, R., Marshall, C. J., Monuki, E. S., Lemke, G. and Richardson, W. D. (1992). Down-regulation of the POU transcription factor SCIP is an early event in oligodendrocyte differentiation in vitro. *Development* **116**, 193-200.

Faus, I., Hsu, H.-J. and Fuchs, E. (1994). Oct-6: a regulator of keratinocyte gene expression in stratified squamous epithelia. *Mol. Cell. Biol.* **14**, 3263-3275.

Frantz, G. D., Bohner, A. P., Akers, R. M. and McConnell, S. K. (1994). Regulation of the POU domain gene SCIP during cerebral cortical development. *J. Neurosci.* **14**, 472-485.

Friede, R. L. and Samorajski, T. (1968). Myelin formation in the sciatic nerve of the rat. A quantitative electron microscopic, histochemical and radioautographic study. *J. Neuropathol. Exp. Neurol.* **27**, 546-570.

Grinspan, J. B., Marchionni, M. A., Reeves, M., Coulaloglou, M. and Scherer, S. S. (1996). Axonal interactions regulate Schwann cell apoptosis in developing peripheral nerve: neuregulin receptors and the role of neuregulins. *J. Neurosci.* **16**, 6107-6118.

Hasel, K. W. and Sutcliffe, J. G. (1990). Nucleotide sequence of a cDNA coding for mouse cyclophilin. *Nucleic Acids Res.* **18**, 4019.

Herr, W. and Cleary, M. A. (1995). The POU domain: versatility in transcriptional regulation by a flexible two-in-one DNA-binding domain. *Genes Dev.* **9**, 1679-1693.

Jaegle, M. and Meijer, D. (1998). Role of Oct-6 in Schwann cell differentiation. *Microsc. Res. Tech.* **41**, 372-378.

Jaegle, M., Mandemakers, W., Broos, L., Zwart, R., Karls, A., Visser, P., Grosveld, F. and Meijer, D. (1996). The POU factor Oct-6 and Schwann cell differentiation. *Science* **273**, 507-510.

Jessen, K. R., Brennan, A., Morgan, L., Mirsky, R., Kent, A., Hashimoto, Y. and Gavrilovic, J. (1994). The Schwann cell precursor and its fate: a study of cell death and differentiation during gliogenesis in rat embryonic nerves. *Neuron* **12**, 509-527.

Krieg, P. A. and Melton, D. A. (1987). In vitro RNA synthesis with SP6 RNA polymerase. *Meth. Enzymol.* **155**, 397-415.

Leger, H., Sock, E., Renner, K., Grummt, F. and Wegner, M. (1995). Functional interaction between the POU domain protein Tst-1/Oct-6 and the high-mobility-group protein HMG-I/Y. *Mol. Cell. Biol.* **15**, 3738-3747.

Lemke, G., Lamar, E. and Patterson, J. (1988) Isolation and analysis of the gene encoding peripheral myelin protein zero. *Neuron* **1**, 73-83.

Martin, J. R. and Webster, H. D. (1973). Mitotic Schwann cells in developing nerve: their changes in shape, fine structure, and axon relationships. *Dev. Biol.* **32**, 417-431.

Messing, A., Behringer, R. R., Hammang, J. P., Palmiter, R. D., Brinster, R. L. and Lemke, G. (1992). P_0 promoter directs expression of reporter and toxin genes to Schwann cells of transgenic mice. *Neuron* **8**, 507-520.

Mirsky, R. and Jessen, K. R. (1996). Schwann cell development, differentiation, and myelination. *Curr. Opin. Neurobiol.* **6**, 89-96.

Monuki, E. S., Kuhn, R. and Lemke, G. (1993). Repression of the myelin P_0 gene by the POU transcription factor SCIP. *Mech. Dev.* **42**, 15-32.

Monuki, E. S., Kuhn, R., Weinmaster, G., Trapp, B. D. and Lemke, G. (1990). Expression and activity of the POU transcription factor SCIP. *Science* **249**, 1300-1303.

Monuki, E. S., Weinmaster, G., Kuhn, R. and Lemke, G. (1989). SCIP: A glial cell POU domain gene regulated by cyclic AMP. *Neuron* **3**, 783-793.

Murphy, P., Topilko, P., Schneider-Maunoury, S., Seitanidou, T., Baron-Van Evercooren, A. and Charnay, P. (1996). The regulation of Krox-20 expression reveals important steps in the control of peripheral glial cell development. *Development* **122**, 2847-2857.

Nakao, J., Shinoda, J., Nakai, Y., Murase, S. and Uyemura, K. (1997). Apoptosis regulates the number of Schwann cells at the premyelinating stage. *J. Neurochem.* **68**, 1853-1862.

Peters, A. and Muir, A. R. (1958). The relationship between axons and Schwann cells during development of peripheral nerves in the rat. *Quart. J. Exp. Physiol.* **44**, 117-130.

Peterson, D. A., Leppert, J. T., Lee, K. F. and Gage, F. H. (1997). Basal forebrain neuronal loss in mice lacking neurotrophin receptor p75 [letter]. *Science* **277**, 837-839.

Peterson, D. A., Lucidi-Phillipi, C. A., Eagle, K. L. and Gage, F. H. (1994). Perforant path damage results in progressive neuronal death and somal atrophy in layer II of entorhinal cortex and functional impairment with increasing postdamage age. *J. Neurosci.* **14**, 6872-6885.

Peterson, D. A., Lucidi-Phillipi, C. A., Murphy, D. P., Ray, J. and Gage, F. H. (1996). Fibroblast growth factor-2 protects entorhinal layer II glutamatergic neurons from axotomy-induced death. *J. Neurosci.* **16**, 886-898.

Sambrook, J., Fritsch, E. F. and Maniatis, T. (1989). *Molecular Cloning: A Laboratory Manual.* Cold Spring Harbor, New York: Cold Spring Harbor Laboratory Press.

Scherer, S. S., Wang, D. Y., Kuhn, R., Lemke, G., Wrabetz, L. and Kamholz, J. (1994). Axons regulate Schwann cell expression of the POU transcription factor SCIP. *J. Neurosci.* **14**, 1930-1942.

Schneider-Maunoury, S., Topilko, P., Seitandou, T., Levi, G., Cohen-Tannoudji, M., Pournin, S., Babinet, C. and Charnay, P. (1993). Disruption of Krox-20 results in alteration of rhombomeres 3 and 5 in the developing hindbrain. *Cell* **75**, 1199-1214.

Schreiber, J., Enderich, J., Sock, E., Schmidt, C., Richter-Landsberg, C. and Wegner, M. (1997). Redundancy of class III POU proteins in the oligodendrocyte lineage. *J. Biol. Chem.* **272**, 32286-32293.

Sereda, M., Griffiths, I., Puhlhofer, A., Stewart, H., Rossner, M. J., Zimmerman, F., Magyar, J. P., Schneider, A., Hund, E., Meinck, H. M. et al. (1996). A transgenic rat model of Charcot-Marie-Tooth disease. *Neuron* **16**, 1049-1060.

Stewart, H. J., Morgan, L., Jessen, K. R. and Mirsky, R. (1993). Changes in DNA synthesis rate in the Schwann cell lineage in vivo are correlated with the precursor—Schwann cell transition and myelination. *Eur. J. Neurosci.* **5**, 1136-1144.

Suzuki, N., Rohdewohld, H., Neuman, T., Gruss, P., and Scholer, H.R. (1990). Oct-6: a POU transcription factor expressed in embryonal stem cells and in the developing brain. *EMBO J.* **9**, 3723-3732.

Swiatek, P. J. and Gridley, T. (1993). Perinatal lethality and defects in hindbrain development in mice homozygous for a targeted mutation of the zinc finger gene Krox20. *Genes Dev.* **7**, 2071-2084.

Syroid, D. E., Maycox, P. R., Burrola, P. G., Liu, N., Wen, D., Lee, K.-F., Lemke, G. and Kilpatrick, T. J. (1996). Cell death in the Schwann cell lineage and its regulation by neuregulin. *Proc. Natl. Acad. Sci. USA* **93**, 9229-9234.

Taylor, V. and Suter, U. (1997). Molecular biology of axon-glia interactions in the peripheral nervous system. *Prog. Nucleic Acid Res. Mol. Biol.* **56**, 225-256.

Thomaidou, D., Mione, M.C., Cavanagh, J.F., and Parnavelas, J.G. (1997). Apoptosis and its relation to the cell cycle in the developing cerebral cortex. *J. Neurosci.* **17**, 1075-85.

Topilko, P., Schneider-Maunoury, S., Levi, G., Baron-Van Evercooren, A., Chennoufi, A. B., Seitanidou, T., Babinet, C. and Charnay, P. (1994). Krox-20 controls myelination in the peripheral nervous system. *Nature* **371**, 796-799.

Trachtenberg, J. T. and Thompson, W. J. (1996). Schwann cell apoptosis at developing neuromuscular junctions is regulated by glial growth factor. *Nature* **379**, 174-177.

Webster, H. D., Martin, R. and O'Connell, M. F. (1973). The relationships between interphase Schwann cells and axons before myelination: a quantitative electron microscopic study. *Dev. Biol.* **32**, 401-416.

Weinstein, D. E., Burrola, P. G. and Lemke, G. (1995). Premature Schwann cell differentiation and hypermyelination in mice expressing a targeted antagonist of the POU transcription factor SCIP. *Mol. Cell. Neurosci.* **6**, 212-229.

West, M. J. (1993). New stereological methods for counting neurons. *Neurobiol. Aging* **14**, 275-285.

West, M. J. and Gundersen, H. J. (1990). Unbiased stereological estimation of the number of neurons in the human hippocampus. *J. Comp. Neurol.* **296**, 1-22.

You, K. H., Hsieh, C. L., Hayes, C., Stahl, N., Francke, U. and Popko, B. (1991). DNA sequence, genomic organization, and chromosomal localization of the mouse peripheral myelin protein zero gene: identification of polymorphic alleles. *Genomics* **9**, 751-757.

Zorick, T. S. and Lemke, G. (1996). Schwann cell differentiation. *Curr. Opin. Cell. Biol.* **8**, 870-876.

Zorick, T. S., Syroid, D. E., Arroyo, E., Scherer, S. S. and Lemke, G. (1996). The transcription factors SCIP and Krox-20 mark distinct stages and cell fates in Schwann cell differentiation. *Mol. Cell. Neurosci.* **8**, 129-146.